

#### Contents lists available at ScienceDirect

## Physica E

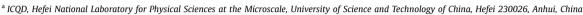
journal homepage: www.elsevier.com/locate/physe



CrossMark

## Coulomb drag in topological insulator films





<sup>&</sup>lt;sup>b</sup> School of Physics, The University of New South Wales, Sydney 2052, Australia

#### HIGHLIGHTS

- Coulomb drag resistivity  $\sim T^2 d^{-4}$ .
- Qualitatively and quantitatively different from graphene.
- Analytical results of limited applicability.

#### ARTICLE INFO

Article history:
Received 28 September 2015
Received in revised form
1 November 2015
Accepted 21 November 2015
Available online 9 December 2015

Keywords: Electron-electron interactions Coulomb drag Topological insulator

#### ABSTRACT

We study Coulomb drag between the top and bottom surfaces of topological insulator films. We derive a kinetic equation for the thin-film spin density matrix containing the full spin structure of the two-layer system, and analyze the electron–electron interaction in detail in order to recover all terms responsible for Coulomb drag. Focusing on typical topological insulator systems, with a film thicknesses d up to 6 nm, we obtain numerical and approximate analytical results for the drag resistivity  $\rho_{\rm D}$  and find that  $\rho_{\rm D}$  is proportional to  $T^2d^{-4}n_{\rm a}^{-3/2}n_{\rm p}^{-3/2}$  at low temperature T and low electron density  $n_{\rm a,p}$ , with a denoting the active layer and p the passive layer. In addition, we compare  $\rho_{\rm D}$  with graphene, identifying qualitative and quantitative differences, and we discuss the multi-valley case, ultra thin films and electron–hole layers.

© 2015 Elsevier B.V. All rights reserved.

#### 1. Introduction

Three-dimensional topological insulators (3DTIs) are a novel class of bulk insulating materials that possess conducting surface states with a chiral spin texture [1–9]. Thanks to their topology, these surface states remain gapless in the presence of time-reversal invariant perturbations. Following their initial observation [10–19], improvements in TI growth have made them suitable for fundamental research [20–23]. Although the reliable identification of the surface states in transport, which remains the key to TIs becoming technologically important, has remained elusive, a number of experiments have successfully identified surface transport signatures in isolated samples. These were initially mostly singled out via quantum oscillations or in gated thin films [18,19,21,22,20]. Recently, four-point transport measurements on clean surfaces in an ultrahigh vacuum have reported a surfacedominated conductivity [24]. A current induced spin polarization also constitutes a signature of surface transport [25,26] and was reported in recent experimental studies [27-29]. Magnetic TIs have also been successfully manufactured [30-32], and the

anomalous [33] and quantum anomalous Hall effects [34,35] have been detected [36–38]. Hybrid structures such as Tl/superconductor junctions have been fabricated [39,40], which are expected to give rise to topological superconductivity and Majorana fermions [41,42].

Transport experiments and theoretical work have mostly focused on longitudinal [43–48] and Hall transport properties [37,49–51], thermoelectric response [52–54] and weak antilocalization [55–58], all essentially single-particle phenomena. The interplay of strong spin–orbit coupling and electron–electron interactions in TIs is at present not completely understood [59–66].

An interaction effect that can be tested experimentally in transport is Coulomb drag, which is caused by the transfer of momentum between electrons in different layers due to the interlayer electron–electron scattering. Coulomb drag has been used for decades as an experimental probe of interactions [67–69], and has recently attracted considerable attention in massless Dirac fermion systems such as graphene [70–83]. Our focus in this paper is on Coulomb drag in TIs with no magnetic impurities. Unlike graphene, the spin and orbital degrees of freedom are coupled by the strong spin–orbit interaction, TIs have an odd number of valleys on a single surface, and the relative permittivity is different, while in known band TIs screening is qualitatively and

<sup>\*</sup> Corresponding author.

quantitatively different, since it does not involve the interplay of the layer and valley degrees of freedom. All these features impact the drag current. We introduce a density matrix method to calculate the Coulomb drag current in topological insulator films, which fully takes into account the spin degree of freedom and interband coherence. The central result of our work is the drag resistivity, which analytically takes the form

$$\rho_{\rm D} = -\frac{\hbar}{e^2} \frac{\zeta(3)}{16\pi} \frac{(k_{\rm B}T)^2}{A^2 r_{\rm s}^2 n_{\rm a}^{3/2} n_{\rm p}^{3/2} d^4},\tag{1}$$

where  $k_{\rm B}$  is the Boltzmann constant, A is the TI spin-orbit constant,  $r_{\rm s}$  is the Wigner-Seitz radius (effective fine structure constant) which represents the ratio of the electrons' average Coulomb potential and kinetic energies, d is the layer separation and  $n_{\rm a,p}$  are the electron densities in the active and passive layers, respectively. For a single-valley system  $r_{\rm s}=e^2/(2\pi\epsilon_0\epsilon_r A)$ , with  $\epsilon_r$  being the relative permittivity. The intralayer resistivity  $\rho_{\rm a,p}=\frac{4\pi\hbar^2}{e^2Ak_{\rm Fa,p}r_{\rm a,p}}$  with  $k_{\rm Fa,p}$  being the Fermi wave vectors.

The outline of this paper is as follows. In Section 2 the interlayer electron-electron scattering matrix is given, including the interlayer screened Coulomb interaction. In Section 3 we derive the kinetic equation of topological insulators for spin density matrices of top and bottom surfaces with the full scattering term in the presence of an arbitrary elastic scattering potential to linear order in the impurity density. In Section 4, we calculate the analytical and numerical expressions of drag resistivity. Our findings are summarized in Section 5, and we also discuss the broader implications of our results and present a comparison with graphene. Section 6 discusses extensions of our theory to treat the multi-valley case and ultra-thin films, and briefly touches upon exciton condensation. Finally, Section 7 contains our conclusions.

#### 2. Electron-electron interaction

The system is described by the many-particle density matrix  $\hat{F}$ , which obeys the quantum Liouville equation [84]

$$\frac{\mathrm{d}\hat{F}}{\mathrm{d}t} + \frac{i}{\hbar}[\hat{H}, \hat{F}] = 0, \tag{2}$$

where  $\hat{H} = \hat{H}^{1e} + \hat{V}^{ee}$  with

$$\hat{H}^{1e} = \sum_{\alpha\beta} H_{\alpha\beta} c_{\alpha}^{\dagger} c_{\beta},$$

$$\hat{V}^{ee} = \frac{1}{2} \sum_{\alpha\beta\gamma\delta} V_{\alpha\beta\gamma\delta}^{ee} c_{\alpha}^{\dagger} c_{\beta}^{\dagger} c_{\gamma} c_{\delta}.$$
(3)

In a two-layer system the indices  $\alpha \equiv k s_k l$  represent the wave vector, band, and layer indices respectively. The band index  $s_k = \pm$  with + representing the conduction band and -the valence band, while the layer index l = (a, p) with 'a' the active layer and 'p' the passive layer. The two-particle matrix element  $V_{\alpha\beta\gamma\delta}^{ee}$  in a basis spanned by a generic set of wave functions  $\{\phi_{\alpha}(\mathbf{r})\}$  is given by

$$V_{\alpha\beta\gamma\delta}^{ee} = \int d\mathbf{r} \int d\mathbf{r}' \, \phi_{\alpha}^{*}(\mathbf{r}) \phi_{\beta}^{*}(\mathbf{r}') V_{\mathbf{r}-\mathbf{r}'}^{ee} \phi_{\delta}(\mathbf{r}) \phi_{\gamma}(\mathbf{r}'), \tag{4}$$

where  $V^{ee}_{r-r'}=rac{e^2}{4\pi\epsilon_0\epsilon_r\,|\,r-r'|}$  is the unscreened Coulomb interaction. The one-particle reduced density matrix is the trace

$$\rho_{\xi\eta} = \operatorname{tr}(c_{\eta}^{\dagger}c_{\xi}\hat{F}) \equiv \langle c_{\eta}^{\dagger}c_{\xi}\rangle \equiv \langle \hat{F}\rangle_{1e}, \tag{5}$$

which satisfies [59]

$$\frac{\mathrm{d}\rho_{\xi\eta}}{\mathrm{d}t} + \frac{i}{\hbar} [\hat{H}_{1e}, \hat{\rho}]_{\xi\eta} = \frac{i}{\hbar} \langle [\hat{V}_{ee}, c_{\eta}^{\dagger} c_{\xi}] \rangle, \tag{6}$$

where the many-electron averages such as  $\langle [\hat{V}_{ee},\,c_{\eta}^{\dagger}c_{\bar{e}}]\rangle$  are factorized as

$$\langle c_{\alpha}^{\dagger} c_{\beta}^{\dagger} c_{\gamma} c_{\delta} \rangle = \langle c_{\alpha}^{\dagger} c_{\delta} \rangle \langle c_{\beta}^{\dagger} c_{\gamma} \rangle - \langle c_{\alpha}^{\dagger} c_{\gamma} \rangle \langle c_{\beta}^{\dagger} c_{\delta} \rangle + G_{\alpha\beta\gamma\delta}. \tag{7}$$

in which we introduce the  $G_{\alpha\beta\gamma\delta}$  as the matrix elements of the twoparticle correlation operator  $\hat{G}$ .  $G_{\alpha\beta\gamma\delta}$  give rise to the electronelectron scattering term in the kinetic equation [84]. The first two terms on the right side of Eq. (7) which represent the Hartree-Fock mean-field part of the electron-electron interactions have been investigated in Ref. [59]. In Ref. [59] it was demonstrated that the electrical current and the nonequilibrium spin polarization undergo a small renormalization due to the mean-field part of electron-electron interactions and are consequently slightly reduced as compared with their non-interacting values. We are not including this weak renormalization here, so the right-hand side of Eq. (6) only gives the electron–electron scattering term  $\hat{\int}_{ee} (\hat{\rho}|t)$ which has two contributions, representing intralayer and interlayer electron-electron scattering. Moreover, since the intralayer electron-electron scattering does not contribute to the drag current, we concentrate on the interlayer electron-electron scattering, for which the scattering term is denoted by  $I^{\text{Inter}}(\hat{\rho}|t)$ . We use below the basis of the eigenstate problem and account for only diagonal part of the density matrix  $J^{\text{Inter}}(f_k) = \langle \mathbf{k} | J^{\text{Inter}}(\hat{\rho} | t) | \mathbf{k} \rangle$ 

$$J^{\text{Inter}}(f_{k}) = \left\langle k \middle| \frac{1}{\hbar^{2}L^{4}} \sum_{qq_{1}} v_{q} v_{q_{1}} \int_{0}^{\infty} dt_{1} e^{\lambda t_{1}} \left[ e^{-iq \cdot r}, \hat{S}(t, t_{1})(1 - \hat{\rho}_{t_{1}}) \right] \right.$$

$$\left. e^{iq_{1}r} \hat{\rho}_{t_{1}} \hat{S}^{+}(t, t_{1}) \left\{ \left\{ e^{iq \cdot r} \hat{S}(t, t_{1}) e^{-iq_{1}r} \hat{\rho}_{t_{1}} \hat{S}^{+}(t, t_{1}) \right\} \right\} \right.$$

$$\left. - \hat{S}(t, t_{1}) \hat{\rho}_{t_{1}} e^{iq_{1}r} (1 - \hat{\rho}_{t_{1}}) \hat{S}^{+}(t, t_{1}) \left\{ \left\{ e^{iq \cdot r} \hat{S}(t, t_{1}) \hat{\rho}_{t_{1}} \right.$$

$$\left. e^{-iq_{1}r} \hat{S}^{+}(t, t_{1}) \right\} \right\} + \hat{S}(t, t_{1}) \left[ \hat{\rho}_{t_{1}}, e^{iq_{1}r} \right] \hat{S}^{+}(t, t_{1})$$

$$\left. \left\{ \left\{ e^{iq \cdot r} \hat{S}(t, t_{1}) \hat{\rho}_{t_{1}} e^{-iq_{1}r} \hat{\rho}_{t_{1}} \hat{S}^{+}(t, t_{1}) \right\} \right\} \right] |k\rangle,$$

$$\left. \left\{ \left\{ e^{iq \cdot r} \hat{S}(t, t_{1}) \hat{\rho}_{t_{1}} e^{-iq_{1}r} \hat{\rho}_{t_{1}} \hat{S}^{+}(t, t_{1}) \right\} \right\} \right] |k\rangle,$$

$$\left. \left\{ \left\{ e^{iq \cdot r} \hat{S}(t, t_{1}) \hat{\rho}_{t_{1}} e^{-iq_{1}r} \hat{\rho}_{t_{1}} \hat{S}^{+}(t, t_{1}) \right\} \right\} \right] |k\rangle,$$

$$\left. \left\{ \left\{ e^{iq \cdot r} \hat{S}(t, t_{1}) \hat{\rho}_{t_{1}} e^{-iq_{1}r} \hat{\rho}_{t_{1}} \hat{S}^{+}(t, t_{1}) \right\} \right\} \right. \right\} |k\rangle,$$

where  $v_q = \frac{e^2}{2\epsilon_0 erq}$ , 1 is the identity matrix,  $L^2$  the area of the 2D system,  $\hat{S}(t,t_1)$  the time evolution operator and  $\{\{\hat{A}\}\} \equiv \hat{A} - \operatorname{tr} \hat{A}$ [84]. The momentum transfer  $\boldsymbol{q} = \boldsymbol{q}_1 = \boldsymbol{k} - \boldsymbol{k}_1 = \boldsymbol{k}_1' - \boldsymbol{k}'$ . Following a series of simplifications, the interlayer Coulomb interaction eventually takes the form  $v_{lk-k_1l}^{(pa)}$ . Without screening  $v_{lk-k_1l}^{(pa)} = v_q e^{-qd}$ . To account for screening, we employ the standard procedure of solving the Dyson equation for the two-layer system in the random phase approximation (RPA) discussed in Ref. [68]. In this approach,  $v_{lk-k_1l}^{(pa)}$  in Eq. (8) becomes the dynamically screened interlayer Coulomb interaction

$$V(\mathbf{q},\omega) = \frac{v_q e^{-qd}}{\epsilon(\mathbf{q},\omega)}.$$
 (9)

The dielectric function of the coupled layer system is

$$\epsilon(\mathbf{q}, \omega) = [1 - \nu_q \Pi_{\mathbf{a}}(\mathbf{q}, \omega)][1 - \nu_q \Pi_{\mathbf{p}}(\mathbf{q}, \omega)] - [\nu_q e^{-qd}]^2 \Pi_{\mathbf{a}}(\mathbf{q}, \omega)$$

$$\Pi_{\mathbf{p}}(\mathbf{q}, \omega), \tag{10}$$

in which the polarization function is obtained by summing the lowest bubble diagram and takes the form

$$\Pi_{l}(\mathbf{q},\omega) = -\frac{1}{L^{2}} \sum_{\mathbf{k}ss'} \frac{F_{s_{\mathbf{k}}s_{\mathbf{k}'}}^{(l)}(f_{0\mathbf{k},s}^{(l)} - f_{0\mathbf{k}',s'}^{(l)})}{\epsilon_{\mathbf{k},s}^{(l)} - \epsilon_{\mathbf{k}',s'}^{(l)} + \hbar\omega + i0^{+}},$$
(11)

### Download English Version:

# https://daneshyari.com/en/article/1543857

Download Persian Version:

https://daneshyari.com/article/1543857

<u>Daneshyari.com</u>